JOURNAL OF Materials CHEMISTRY

# Supercritical fluid processing: a new route for materials synthesis†

**François Cansell,* Bernard Chevalier, Alain Demourgues, Jean Etourneau, Christophe Even, Yves Garrabos, Vincent Pessey, Stéphane Petit, Alain Tressaud and François Weill**

*Institut de Chimie de la Matière Condensée de Bordeaux [ICMCB], CNRS—UPR 9048, Université Bordeaux I, Château Brivazac, Av. du Dr. Schweitzer, 33608 Pessac Cedex, France. E-mail: cansell@chimsol.icmcb.u-bordeaux.fr*

***Received 23rd April 1998, Accepted 29th June 1998***

Supercritical fluids exhibit a range of unusual properties that can be exploited for new reactions which are qualitatively different from those involving classical solid state chemistry. After giving a brief introduction to these fluids we describe their use in inorganic chemistry and related fields. We then present two examples concerning different areas of solid state chemistry: (i) the formation of novel inorganic nanoparticles; (ii) the preparation of new open-structure oxy(hydroxy)fluorides, thus showing the advantages of this supercritical fluid processing that can be seen as an alternative method to regular solution chemistry or solid–gas reactions.

## Introduction

A fluid is in the supercritical domain when both pressure and temperature are above their critical values, $P_c$ and $T_c$. In practice, this definition is restricted to fluids close to their critical points and, hence, with their density close to $\rho_c$. There are numerous fluids for which the critical temperature is moderate. A selection of the most usual ones is listed in Table 1.[1]

Nowadays supercritical fluids are widely used in many fields.[2–4] These fluids are very attractive for materials processing[5] and more particularly for the formation of particles, fibres, thin films (pharmaceuticals, explosives, coatings)[6–9] and for drying materials (highly porous gels).[10,11] Furthermore, these fluid processes are already used in many other applications, such as: separation (petroleum-chemistry separation and purification, food industry);[12–15] chromatography (analytical and preparative separation, determination of physicochemical properties);[16,17] chemical reactivity (low-density polyethylene, waste destruction, polymer recycling);[18–22] and earth sciences (volcanism, geothermal energy, hydrothermal synthesis).[23]

Both the capability of some supercritical fluids to replace toxic industrial solvents and the ability of tuning solvent characteristics for highly specific separations or reactions lead to the current industrial and scientific interest in supercritical fluids.[24] These fluids possess physicochemical properties, such as density, viscosity and diffusivity, which are intermediate between those of liquids and gases (Table 2). The main interest in supercritical fluids as reaction media relies on their continuously adjustable properties from gas to liquid with small pressure and temperature variations. Fig. 1 shows that it is possible to move continuously from the liquid to the gaseous state without crossing the liquid–gas equilibrium line.

Classically, materials preparation in supercritical fluid can be described in three steps: step one: solubilization of solutes in dense fluid (close to the liquid phase) since the solute solubility varies generally as a power law with respect to density;[25] step two: chemical or physical transformation of fluids in the supercritical domain, characterized by specific properties (Table 2);[26,27] step three: materials recovery in the low density fluid domain (close to the gas phase) in order to obtain dry materials.

†Basis of the presentation given at Materials Chemistry Discussion No. 1, 24–26 September 1998, ICMCB, University of Bordeaux, France.

Thus, it is possible to prepare new materials under mild conditions by using either physical or chemical transformations (see Fig. 2). The main results concerning these two possibilities are reported herein. However, first of all, it should be pointed out that supercritical fluids are used in order to provide contaminant-free compounds. Moreover, this method allows one to obtain solid particles exhibiting both a narrow range of size distribution (micronic and nanometric) and specific features (*e.g.* well defined stoichiometry, structure, *etc.*).

## Physical transformations

Concerning the physical transformations, three main techniques are successively presented: the rapid expansion of a supercritical solution (RESS), supercritical antisolvent precipitation: gas anti-solvent (GAS), and precipitation with compressed anti-solvent (PCA).

**Table 1** Critical coordinates of usual pure fluids. $T_c$, $P_c$ and $\rho_c$ are the critical temperature, pressure and density, respectively[1]

| Fluid | $T_c$/°C | $P_c$/MPa | $\rho_c$/kg m$^{-3}$ |
|---|---|---|---|
| Carbon dioxide | 31.2 | 7.38 | 468 |
| Ammonia | 132.4 | 11.29 | 235 |
| Water | 374.1 | 22.1 | 317 |
| Ethylene | 9.5 | 5.06 | 220 |
| Ethane | 32.5 | 4.91 | 212 |
| Propane | 96.8 | 4.26 | 225 |
| *n*-Pentane | 196.6 | 3.37 | 232 |
| Cyclohexane | 279.9 | 4.03 | 270 |
| Methanol | 240.0 | 7.95 | 275 |
| Ethanol | 243.1 | 6.39 | 280 |
| Isopropanol | 235.6 | 5.37 | 274 |
| Acetone | 235.0 | 4.76 | 273 |

**Table 2** Characteristic magnitudes of thermophysical properties of fluids

| | Liquid | Supercritical fluid | Gas[a] |
|---|---|---|---|
| $\rho$/kg m$^{-3}$ | 1000 | 100–800 | 1 |
| $\eta$/Pa s | $10^{-3}$ | $10^{-4}$–$10^{-5}$ | $10^{-5}$ |
| $D^b$/m$^2$ s$^{-1}$ | $10^{-9}$ | $10^{-8}$ | $10^{-5}$ |

$\rho$ = density; $\eta$ = viscosity; $D$ = diffusion coefficient. [a]At ambient conditions. [b]For small-molecule solute.

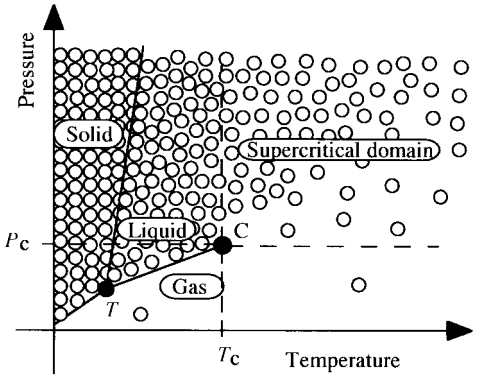


**Fig. 1** Schematic representation of a phase diagram illustrating the density evolution from the liquid to the gas without crossing the T–C line which corresponds to the liquid–gas equilibrium line, C being the critical point and T being the triple point. $P_c$ and $T_c$ are the critical pressure and temperature respectively.

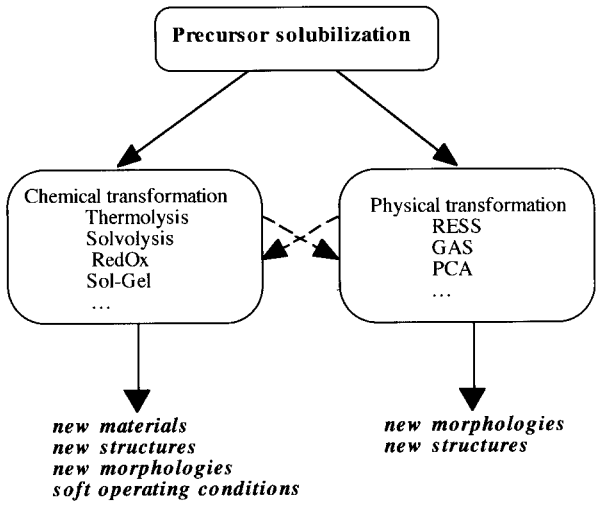


**Fig. 2** Possible routes for material elaboration using supercritical fluids. RESS = rapid expansion of supercritical solution; GAS = gas anti-solvent recrystallisation; PCA = precipitation with compressed anti-solvent.

### Rapid expansion of supercritical solution (RESS) process

In this process, the reactant is first solubilized in a supercritical fluid which is then expanded across a nozzle or a capillary at a very high velocity. Such a rapid expansion leads to a high solute supersaturation and subsequently to the precipitation of small monodispersed particles.[28] This process has been applied to inorganic,[29] organic[30] and pharmaceutical[31] compounds. It allows the preparation of either an intimately mixed powder of two inorganic compounds (*e.g.* $SiO_2$ and KI) or an inorganic and organic combination [*e.g.* KI and poly(vinyl chloride)].[32]

The major limitation of the RESS process is the low solubility of many compounds in supercritical fluids. For example in carbon dioxide, the solute solubilities are about 0.01 wt.% or less. The other challenge for large commercial plant configuration is associated with nozzle design in order to avoid particle accumulation and the freezing caused by the rapid expansion.

### Supercritical anti-solvent precipitation processes: gas anti-solvent (GAS) and precipitation with compressed anti-solvent (PCA)

In these processes a solute is dissolved in an organic solvent. The addition of a supercritical fluid leads to a lower solubility of the solute in the liquid phase since the supercritical fluid remains soluble in the organic solvent. These processes are used for explosives, polymers, food, pharmaceutical compounds, coloring matter and catalysts. For the latter it can be specified that zinc acetate nanoparticles down to about 30 nm are obtained with an average particle size of 50 nm.[33]

With the GAS process, a batch of the solution (solute dissolved in organic solvent) with dense carbon dioxide for example, is expanded several times in a vessel. Because of the lower solvent strength of the carbon dioxide–expanded solvent mixture, the fluid medium becomes supersaturated, thus forcing the solute to precipitate in microparticles.

The PCA process consists of spraying the solution through a nozzle into dense carbon dioxide, for example.

These two processes allow the control of the particle size (micronic and submicronic). Unfortunately their use is limited by the separation of the solid particles from the solvents.

## Chemical transformations

Physico-chemical properties of supercritical fluids as a reactive medium are relatively easy to adjust by operating conditions. Indeed, these tunable characteristics, such as density, viscosity, and diffusivity, influence directly the reaction rate constants. For the reactions involving ionic species, the variations of the relative permittivity and of the ion products influence both the chemical equilibrium and the evolution of the transition state. By moving continuously from the liquid to the gaseous state, the efficiency of the reaction may be significantly enhanced to create a completely new chemical process.

As the reactivity of organic compounds in supercritical fluids has already been intensively studied,[34,35] we focused on materials preparation. Supercritical fluids are used for matter transport or as chemical media in order to produce submicronic particles, compounds with specific features, polymer–metal composites, aerogels and thin films. Chemical reactions generally involve the thermal decomposition of a metal-containing precursor. The various applications developed in the field of inorganic materials are also reported.

### Oxide nanoparticles

Submicronic $TiO_2$ powder has been obtained in a flow reactor by a sol–gel process. Titanium isopropoxide, $Ti(O\text{-}iC_3H_7)_4$, is hydrolytically decomposed by water, produced by the catalytic dehydration of the isopropyl alcohol used as the supercritical solvent.[36] Titanium hydroxides are formed and their decomposition into $TiO_2$ kinetically limits the reaction. At temperature and pressure around 300 °C and 10 MPa respectively, particles with a narrow range of size distribution (20–60 nm), some of which crystallize with the anatase structure, are weakly associated into spherical agglomerates (500–2000 nm). A model of the flow reactor, has been made including hydrodynamic and kinetic studies,[37] and experimentally validated for optimizing the process.

Metal oxide submicronic particles can also be obtained in supercritical water by the hydrolysis of metal salts in aqueous solutions. Numerous oxides have been studied such as $Fe_2O_3$, $Co_3O_4$, NiO, $ZrO_2$, $TiO_2$ and $CeO_2$.[38] In the case of $TiO_2$, $TiCl_4$ was used as the precursor and leads, at 30 MPa and 400–450 °C, to the formation of $TiO_2$ (anatase) with a prismatic shape and a size of 20 nm.[39]

Porous substrates (alumina or zirconia) with high surface areas have been impregnated with supercritical solutions of metal salts (carbonate, acetate, *etc.*), which can be adsorbed or deposited as a film on the surface of the substrate by lowering the pressure.[40]

Supercritical fluid has also been used as a drying medium in the sol–gel process for the preparation of nanometric tin oxide particles (3–5 nm).[41]

### Metal nanoparticles

Micronic metallic powders (as pure metals, metal alloys, or mixtures thereof) have been prepared from metal salts.[42] Precursors are solubilized in methanol at a temperature lower than that employed to generate a metallic powder. As an example, micronic Cu particles were obtained from a solution of $Cu(OAc)_2$ at 275 °C and about 14 MPa. When $Pd(OAc)_2$ was added to a methanol solution of $Cu(OAc)_2$, a mixture of Pd and Cu metals and a face centered cubic Cu–Pd alloy were obtained; both systems were identified by XRD and ESCA measurements.

### Compounds with specific features

Semiconducting quaternary antimony sulfides, such as $KAg_2SbS_4$ or $RbAg_2SbS_4$, have been prepared in supercritical ammonia at 160 °C and about 22 MPa during 4 days from the appropriate mole ratio of $K_2S_4$, $K_2CO_3$ or $Rb_2CO_3$ with Ag, $Sb_2S_3$ and $S_8$. The use of supercritical ammonia leads to high quality crystal growth, owing to its specific transport properties (viscosity, solubility, *etc.*).[43]

### Polymer–metal composites

Polymer–metal composites consist of isolated nanoclusters of metal atoms distributed homogeneously throughout polymeric substrates. For example, a metal precursor such as dimethyl(cycloocta-1,4-diene)platinum(II) is dissolved in supercritical carbon dioxide and impregnated into the polymer [poly(4-methylpent-1-ene)]. Thermolytic reduction of the precursor in the $CO_2$-swollen polymer medium at 140 °C and under 26 MPa pressure produces platinum aggregates with a maximum diameter of approximately 50 nm.[44]

### Aerogels

Sol–gel reactions have been directly performed in supercritical carbon dioxide as a reactive medium by using formic acid as condensation reagent.[45] Supercritical carbon dioxide appears to be a better solvent than ethanol for preparing phenylene-bridged polysilsesquioxane aerogels from 1,4-bis(triethoxysilyl)benzene. In addition, this process can be successfully used to generate monolithic aerogels from their precursors in a single step.

### Thin films

Supercritical fluid transport and chemical deposition can be used for the formation of thin films on a substrate. This film deposition technique can use nonvolatile precursors, unlike the chemical vapor deposition process. In supercritical fluid transport and chemical deposition technique, precursors are dissolved in the supercritical fluid. Then, this solution flows through a restrictor into a deposition chamber where the rapid expansion of the supercritical fluid causes the vaporisation of the solutes. The precursors can be decomposed at or near a substrate surface to form a thin film. This leads to the formation of pure metal (*e.g.* Al, Cr, Ni, Cu, *etc.*), or oxide (*e.g.* CuO, $SiO_2$, $Cr_2O_3$, *etc.*) films. Moreover, the stoichiometric ratios of the precursors for multi-element coatings (*e.g.* $YBa_2Cu_3O_{7-x}$) can be precisely controlled.[46–48]

After this brief review, we present our own results concerning a new route for nanoparticle formation and for the synthesis of new phases in solid state chemistry such as open-structure oxy(hydroxy)fluorides.

## Preparation of nanoparticles

The aim of this work is to develop a new method for the preparation of nanoparticles. Indeed, metallic nanoparticles with dimensions of tens of nanometers or less exhibit size-dependent electrical, chemical and magnetic properties. The chemical transformation of metallic precursors inside a supercritical fluid is a new route for obtaining nanometric homogeneous powders. The process mainly deals with the dissolution of precursors in a dense fluid, followed by the decomposition of the precursors in supercritical fluid for preparing either powders or thin films of materials.

### Experimental setup

The apparatus used for chemical synthesis in supercritical fluid media is shown in Fig. 3. The system itself, placed in a temperature controlled hot-air oven, is composed of: (i) two high pressure 316 stainless steel cells. The first one (cell A) is the mass exchanger. It is a cylinder of 1.8 cm diameter and 5.5 cm length filled with a glass packed bed of 0.2 cm diameter. A glass wool plug is placed at the outlet of the cylinder in order to avoid the dragging of the precursor by the flowing fluid. For each experimental run the cylinder is charged with 1 g of the precursor. The second cell (cell B) is the reactor. It consists of a cylinder of 1.8 cm diameter and 9.5 cm length. An external heating resistor allows the generation of a flash of temperature. A glass wool plug is placed at the outlet of the cylinder for the reasons mentioned above. A polytetrafluoroethylene film (PTFE, 0.25 mm thickness) rolled up inside the cell is used for collecting the metallic particles. (ii) A high pressure generator, which is a fluid metering pump (CM 3200 P/F). This pump provides either constant flow or constant pressure. Only one fluid can be used with this system (in our case it is ammonia). The working pressure is monitored by a digital gauge. (iii) Two thermocouples measure the temperature, one is placed inside the hot-air oven, the other one is inside cell B.

Acetylacetonates of metals [$Cu(AcAc)_2$ and $Fe(AcAc)_3$] were used as precursors. They were all provided by Sigma-

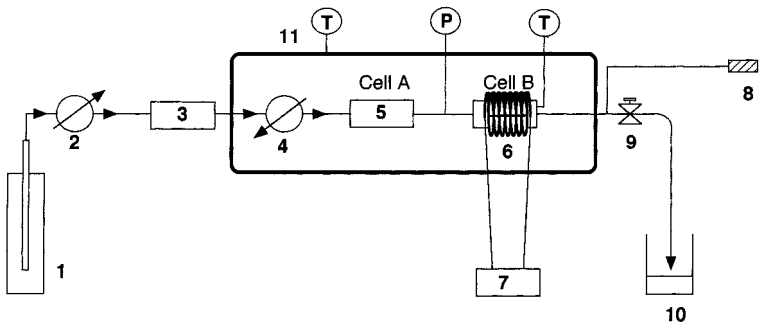


**Fig. 3** Apparatus for chemical synthesis in supercritical fluid media. 1, Fluid tank. 2, Cooling system. 3, High pressure pump: 1–10 ml $min^{-1}$; 0–40 MPa. 4, Heat exchanger. 5, Mass exchanger (cell A). 6, Reactor (cell B). 7, Temperature regulator. 8, Contact breacker. 9, Micrometric valve. 10, Solvent trap. 11, Oven.

Aldrich and used without further purification. Their solubility in ammonia was measured and is reported in Table 3.

The solid particle formation results from the solute thermal decomposition in the supercritical fluid medium. The fact that the critical temperature of this solvent must be lower than that of the metal chelate decomposition justifies the choice of ammonia as the supercritical fluid. In addition this fluid exhibits a high reducing power.

A known amount of precursor is placed in cell A. The system is filled with solvent. Then the hot-air oven is heated at a temperature $T_A$ which allows good solute solubility. Cell B is heated at temperature $T_B$ which allows chemical reaction. When both temperatures are stabilized, the pressure is increased up to 17 MPa and then maintained constant. In these conditions ammonia is liquid in the mass exchanger (cell A) and is in the supercritical domain in the reactor (cell B).

Then the fluid flow rate is stabilized at the working value of 3 ml $min^{-1}$ and the fluid mixture (solvent + precursor) is transported to the reactor. The solute is thermally decomposed in the reactor and the metallic part is precipitated on the PTFE film. The organic part, still soluble in the supercritical solvent, is trapped at the outlet of the installation.

## Results and discussion

Chemical syntheses in supercritical fluids are known to allow the obtention of powders with small particle size and narrow distribution range. Indeed, these syntheses are based on homogeneous nucleation and large supersaturation in a supercritical solvent and the size of the collected particles is very sensitive to the supersaturation: the higher the supersaturation, the smaller the particles.[49] Moreover, in a supercritical fluid small changes of pressure give rise to large changes in both density and solubility.[50] Thereby the optimization of working pressure and temperature in the reactor allows the achievement of high supersaturation and the formation of nanosized particles. This is demonstrated by our results, obtained from the thermal decomposition of $Fe(AcAc)_3$ made in the dense fluid domain and in the supercritical domain. Obviously, supercritical fluids as reactive media allow the formation of smaller particles (with $\phi_{average} = 50$ nm, see Fig. 4) than those obtained in dense fluids (with $\phi_{average} = 800$ nm, see Fig. 5). The experiments have shown that the final particle size depends on the variations of the working conditions ($T$, $P$, solute supersaturation, hydrodynamics, *etc.*). The relationship between size and working conditions is under study.

A solvolysis reaction occurs during the decomposition of the precursor. Indeed, the particle reactivity is very high and thus the use of ammonia may lead to metal nitrides. In the case of $Cu(AcAc)_2$ and $Fe(AcAc)_3$ precursors, we have prepared particles of copper nitride $Cu_3N$ at 200 °C and 17 MPa and iron nitride $Fe_4N$ at 180 °C and 16 MPa (Table 4). The sample of $Cu_3N$ has been characterized by XRD. The pattern indicates that the $Cu_3N$ phase is obtained with copper as impurity (Fig. 6). In the case of the $Fe(AcAc)_3$ decomposition, a mixture of both iron nitride $Fe_4N$ and iron oxide $Fe_2O_3$ was observed (Table 4). This mixture has been characterized by electron diffraction because this sample seems to be amorphous to X-ray diffraction (Fig. 7, Table 5).

**Table 3** Solubility (at 90 °C and 10 MPa) and decomposition temperature (at 16 MPa) values for $Cu(AcAc)_2$ and $Fe(AcAc)_3$ in ammonia (the critical coordinates of ammonia are $T_c = 132.4$ °C and $P_c = 11.29$ MPa)

| | Solubility/g $g^{-1}$ [a] | Decomposition temperature/°C |
|---|---|---|
| $Cu(AcAc)_2$ | $5.8 \times 10^{-3}$ | 190 |
| $Fe(AcAc)_3$ | $3.8 \times 10^{-3}$ | 170 |

[a]Gram of precursor per gram of fluid.

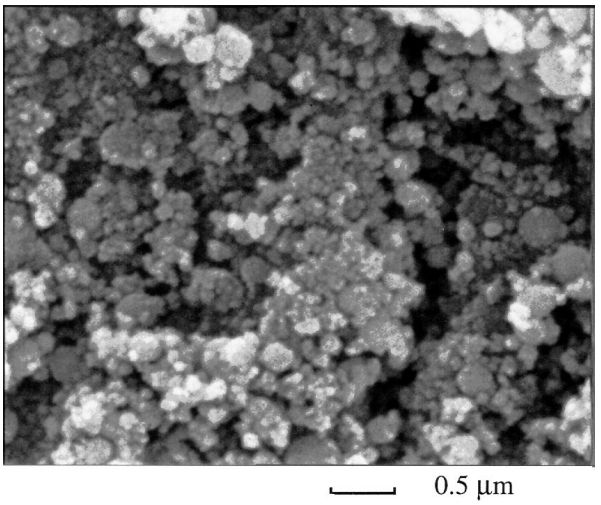


**Fig. 4** SEM picture of the mixture of $Fe_4N$ and $Fe_2O_3$ obtained by the decomposition of $Fe(AcAc)_3$ in supercritical ammonia. ($T_{reactor} = 180$ °C; $P = 16$ MPa).

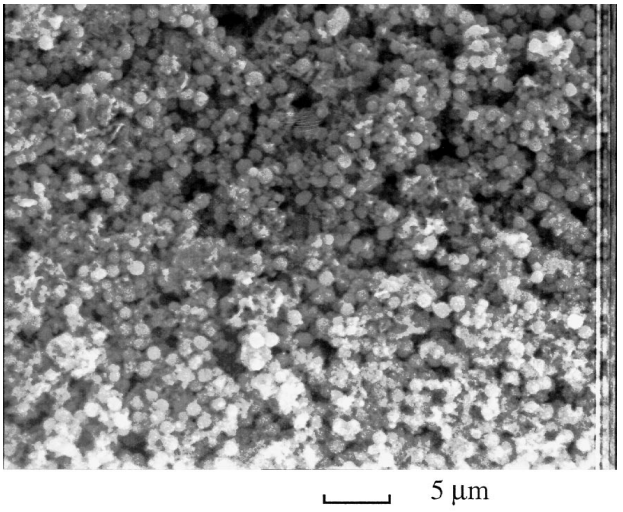


**Fig. 5** SEM picture of the mixture of $Fe_4N$ and $Fe_2O_3$ obtained by the decomposition of $Fe(AcAc)_3$ in liquid ammonia. ($T_{reactor} = 120$ °C; P = 10 MPa.)

**Table 4** Cu and Fe nitride formation in supercritical ammonia

| Precursor | Working conditions | Products |
|---|---|---|
| $Cu(AcAc)_2$ | $T_{mass\ exchanger} = 90$ °C<br>$T_{reactor} = 200$ °C<br>$P = 17$ MPa<br>Ammonia flow = 3 ml $min^{-1}$ | $Cu_3N$ with copper as impurity |
| $Fe(AcAc)_3$ | $T_{mass\ exchanger} = 90$ °C<br>$T_{reactor} = 180$ °C<br>$P = 16$ MPa<br>Ammonia flow = 3 ml $min^{-1}$ | Mixture of $Fe_4N$ and $Fe_2O_3$ |

Aggregates of 50 nm are obtained in the case of the $Fe_4N$–$Fe_2O_3$ mixture. They consist of very small particles ($\leqslant 10$ nm) with a narrow range of size distribution as shown in Fig. 8. The iron oxide formation could be due to the high reactivity of iron with oxygen present in the acetylacetonate groups. New precursors free from oxygen are under study in order to obtain metallic nanoparticles only.

It must be pointed out that our working temperatures for obtaining metal nitrides are clearly lower than those used in classical solid state chemistry routes. Classical ways for making transition-metal nitrides involve high-temperature and high-

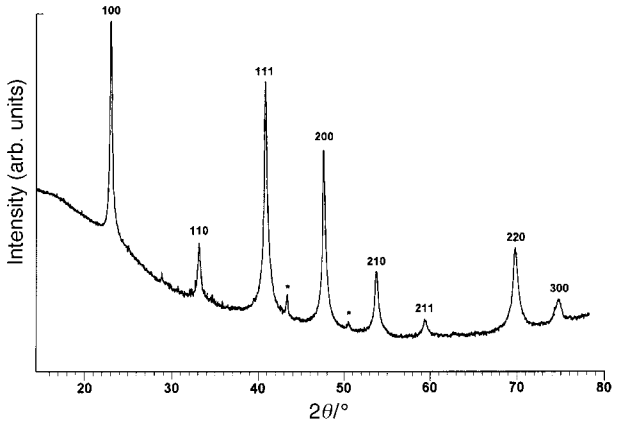


**Fig. 6** X-Ray diffraction pattern of $Cu_3N$ obtained by the decomposition of $Cu(AcAc)_2$ in supercritical ammonia ($T_{reactor}=200\,^{\circ}C$; $P=17$ MPa.) *indicate the peaks relating to copper.

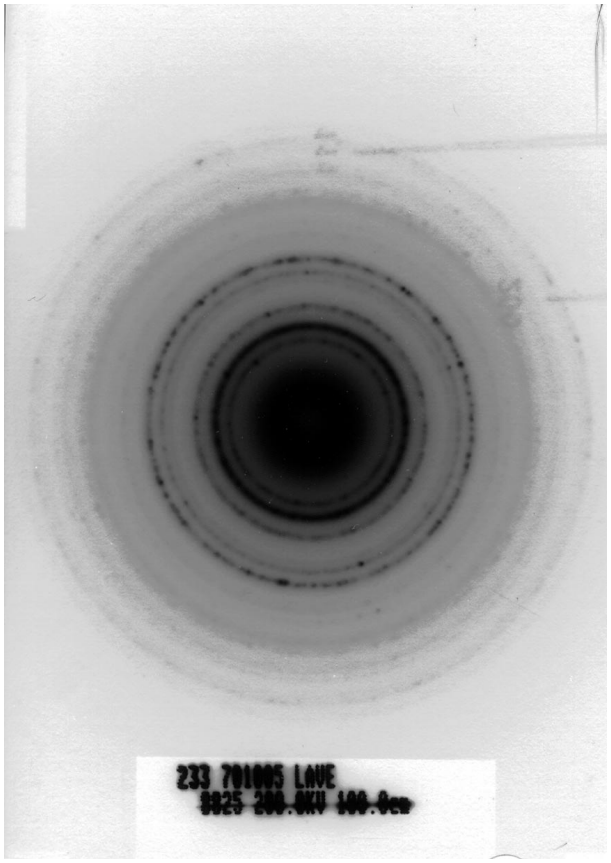

**Fig. 7** Electron diffraction pattern of the mixture of $Fe_4N$ and $Fe_2O_3$ obtained by the decomposition of $Fe(AcAc)_3$ in supercritical ammonia ($T_{reactor}=180\,^{\circ}C$; $P=16$ MPa). (See Table 5.)

pressure reactions between a pure metal and a nitrogen source.[51] However, there are other ways to obtain metal nitrides, based on the use of precursors (such as organometallics, acetates, salts *etc.*). In this case, the working conditions are lowered. Indeed, single crystalline $\gamma'$-$Fe_4N$ can be obtained by chemical transport from iron over $[Fe(NH_3)_6]I_2]$ in supercritical ammonia ($p(NH_3)=600$–$800$ MPa, $460\,^{\circ}C \leqslant T \leqslant 580\,^{\circ}C$)].[52] By heating $CuF_2$ at $280\,^{\circ}C$ in $NH_3$, pure $Cu_3N$ is obtained.[53]

## Open-structure oxy(hydroxy)fluorides

During the past few years, much work has been devoted to the study of heterogeneous catalytic systems. In many reactions, the electrical properties of the catalyst constitute one of the key features, in particular when the materials show mixed conductivity, *i.e.* fast transport of ions in addition to electronic conductivity at various temperatures. In the case of oxides, for instance, ionic conductivity is generally due to polarizing cationic species such as $H^+$ and $Li^+$, or polarisable anionic $O^{2-}/O^-$ entities. The aim of this work was then to elaborate and to study some ($O^{2-}$, $OH^-$, $F^-$) mixed-anion systems showing good mixed conductivity, such as $Sr(OH)X$ ($X=Cl$, Br, I)[54] phases, which are known as protonic conductors.

From a chemical point of view, it was interesting to use transition metal fluorides as starting materials, *i.e.* compounds which already contain ionic M—F bonds, instead of substituting oxy- or hydroxy-anions by fluorine in oxides or hydroxides exhibiting stronger M—O (OH) bonds as was done in previous work.[55,56] From a structural point of view, and in order to produce good catalytic properties, we were rather interested in open structures based on transition metal networks, such as tunnelled or layered frameworks, to enhance the ionic conductivity and to favor electronic conductivity.

A suitable method would then consist of partial hydrolysis in the case of a transition metal fluoride with the desired oxidation state, such as $FeF_3$, whereas oxidative hydrolysis would occur for compounds with lower oxidation states, such as $FeF_2$. We could also consider ternary fluorides such as $NH_4FeF_3$ from which ammonium ions could be topotactically deintercalated, thus entailing the replacement of $F^-$ by $OH^-/O^{2-}$ ions in an aqueous medium, in order to obtain an oxyfluoride or an oxy(hydroxy)fluoride.

**Table 5** *d*-Values obtained for mixture of $Fe_4N$ and $Fe_2O_3$ (see Fig. 7)

| $d_{measured}$/Å | $d_{Fe_4N}$/Å[a] | $d_{Fe_2O_3}$/Å[a] |
|---|---|---|
| | | 6.47 |
| 4.76 | | 4.76 |
| | | 4.01 |
| | 3.79 | |
| | | 3.34 |
| | | 3.24 |
| | | 3.15 |
| 2.99 | | 2.981 |
| | | 2.804 |
| | | 2.728 |
| | 2.684 | |
| 2.55 | | 2.573 |
| | | 2.548 |
| | | 2.458 |
| | | 2.372 |
| | | 2.295 |
| | | 2.243 |
| 2.19 | 2.191 | |
| | | 2.176 |
| | | 2.018 |
| | | 1.997 |
| | | 1.983 |
| | | 1.973 |
| | | 1.897 |
| | | 1.855 |
| | | 1.807 |
| 1.75 | | 1.735 |
| | 1.697 | |
| 1.66 | | 1.666 |
| | | 1.58 |
| 1.53 | 1.549 | |
| 1.31 | 1.342 | |
| 1.25 | 1.265 | |
| | 1.200 | |
| 1.12 | 1.144 | |
| | 1.095 | |
| 1.06 | 1.053 | |
| 1.01 | 1.014 | |
| 0.98 | 0.949 | |
| 0.88 | | |

[a]From ASTM files.

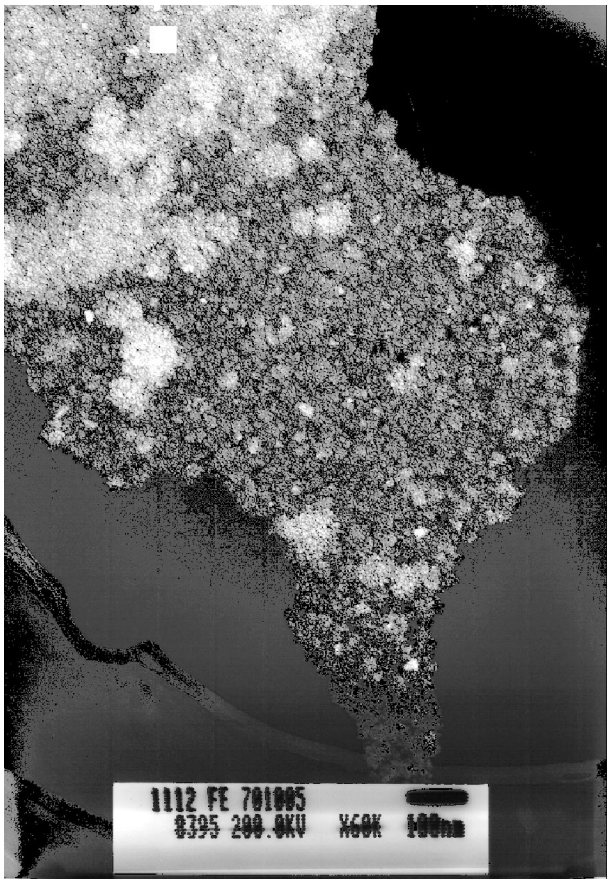


**Fig. 8** TEM picture of the mixture of $Fe_4N$ and $Fe_2O_3$ obtained by the decomposition of $Fe(AcAc)_3$ in supercritical ammonia ($T_{reactor}=180\,^{\circ}C$; $P=16$ MPa).

Unfortunately, several drawbacks arise from these methods: first, fluoride materials are generally sensitive to moisture; secondly, moderate temperatures, necessary to obtain open-structure materials, generally lead to low diffusion of the reactive species (gaseous or liquid) through the solid fluoride material, and then induce a gradient in the chemical composition of the final product.

Therefore, we have chosen to use a supercritical medium which allows very high diffusivity of the species through the transition metal fluorides and good elimination of water. Supercritical $CO_2$ ($scCO_2$) with ethanol as a co-solvent appeared to be a good candidate.

In order to demonstrate the interest and capability of this method for preparing 3d-transition metal oxyfluorides, we focused our attention on iron-based compounds, owing to the well known stability of the two oxidation states $+II$ ($3d^6$) and $+III$ ($3d^5$) present in iron oxides and fluorides. In addition, several attempts were made over the last few decades to prepare iron oxyfluorides with open frameworks.[57] It should be pointed out that only the rutile form of FeOF (Fig. 9a) has been obtained so far, by high temperature reaction.[58,59]

Numerous works have also been reported concerning an iron oxyhydroxide exhibiting an open structure (hollandite type): β-FeOOH.[60,61] This compound was obtained by hydrolysis of $FeCl_3$.[62–64] It has been shown that residual $Cl^-$ anions are always present in the tunnels of the framework, keeping it from collapsing.[65] Some attempts have been made to prepare the corresponding fluorinated phase $FeO(OH)_{1-\varepsilon}F_\varepsilon$ *via* the hydrolysis of $FeF_3$. The material contained only a few atom% of $F^-$ anions which were located in the tunnel sites of the structure.[60] Other authors tried to synthesize such compounds by the hydrolysis of iron hydroxides[56] or nitrates[55,66] in a concentrated NaF or $NH_4F$ aqueous solution, and obtained a higher fluorine content; however it was limited to $\varepsilon<0.3$.

A method for preparing oxy(hydroxy)fluorides with the hollandite-type structure which would lead to a much higher fluorine content, involves the oxidation of transition metal fluorides with $H_2O_2$ solutions. Using this route, we could expect that $F^-$ and $OH^-$ would occupy the same type of sites within the network, at the corners of the $FeX_6$ octahedra, instead of being present only as inserted species in the tunnels of the framework. In this connection we describe here the oxidative hydrolysis of the fluoroperovskite $NH_4FeF_3$ under supercritical conditions.

## Experimental setup

Our experiments were carried out in $scCO_2$; a second high pressure pump was added for the injection of the solution ($H_2O_2$–$H_2O$–ethanol) at temperatures between 50 and 250 °C approximately, and at pressures varying from 10 to 40 MPa. The reactant used was a concentrated aqueous solution of hydrogen peroxide ($H_2O_2$, 30 M), diluted in an equal volume of ethanol. The stainless steel reactor (5 mm diameter, 50 mm long) (cell A of Fig. 3) was prepared as described above and filled with freshly ground $NH_4FeF_3$ powder in a dry argon glove box. It was subsequently mounted on the pressure line in a programmable hot-air oven. The line was then flushed with $CO_2$ before raising the temperature and starting the reaction.

During the treatment, great care should be taken in keeping the system in supercritical conditions in order to avoid water separation: water solubility in $scCO_2$ remains low, and the introduction of large quantities of water would lead to a two-phase system.

After the reaction, the reactor was flushed again with $scCO_2$ in order to eliminate residual water.

The compounds obtained were characterized by electron probe microanalysis (EPMA) (O/Fe and F/Fe ratios), TGA–DTA coupled with mass spectrometry (adsorbed $H_2O$, OH and F contents), diffuse reflectance-IR, electron microscopy (morphology of the particles) and X-ray diffraction.

## Results and discussion

The oxidative process using the water–ethanol solution of $H_2O_2$ in $scCO_2$ on $NH_4FeF_3$ allowed us to prepare oxy(hydroxy)fluorides with the general formula $FeOF_{1-x}(OH)_x\cdot nH_2O$ ($x\leqslant 0.2$, $n\leqslant 0.4$), isostructural with β-FeOOH, *i.e.* exhibiting the hollandite-type structure (Fig. 9b). The frameworks of the rutile-type and the hollandite-type structures are built of chains of octahedra sharing opposite edges (Fig. 9). In the case of the rutile structure, single chains are connected to one other by vertices, whereas in the hollandite structure double chains sharing edges form large square tunnels of about $2\times 0.5$ nm section and running along the $c$ direction. The small amount of water which is present in the compounds mainly depends on the conditions of the final $CO_2$ treatment, performed after the reaction.

After optimization of the experimental supercritical conditions, $NH_4FeF_3$ was treated at 150 °C for 30 min under a $scCO_2$ pressure of 30 MPa. The volume of the injected $H_2O_2$ solution (as described above) was 15 ml. The X-ray diffraction pattern shows a well crystallized single phase with a hollandite-type structure (sample A; Fig. 10a). The tetragonal cell parameters ($a=1.036$ nm, $c=0.302$ nm) are slightly smaller than those reported for β-FeOOH[57] ($a=1.053$ nm, $c=0.303$ nm). The lower $a$-value could be related to the presence of $F^-$ anions instead of $OH^-$ in the framework.

We have also prepared, using the standard hydrolysis route, two other compounds also exhibiting the same hollandite structure: a slightly chlorinated hydrated iron oxyhydroxide

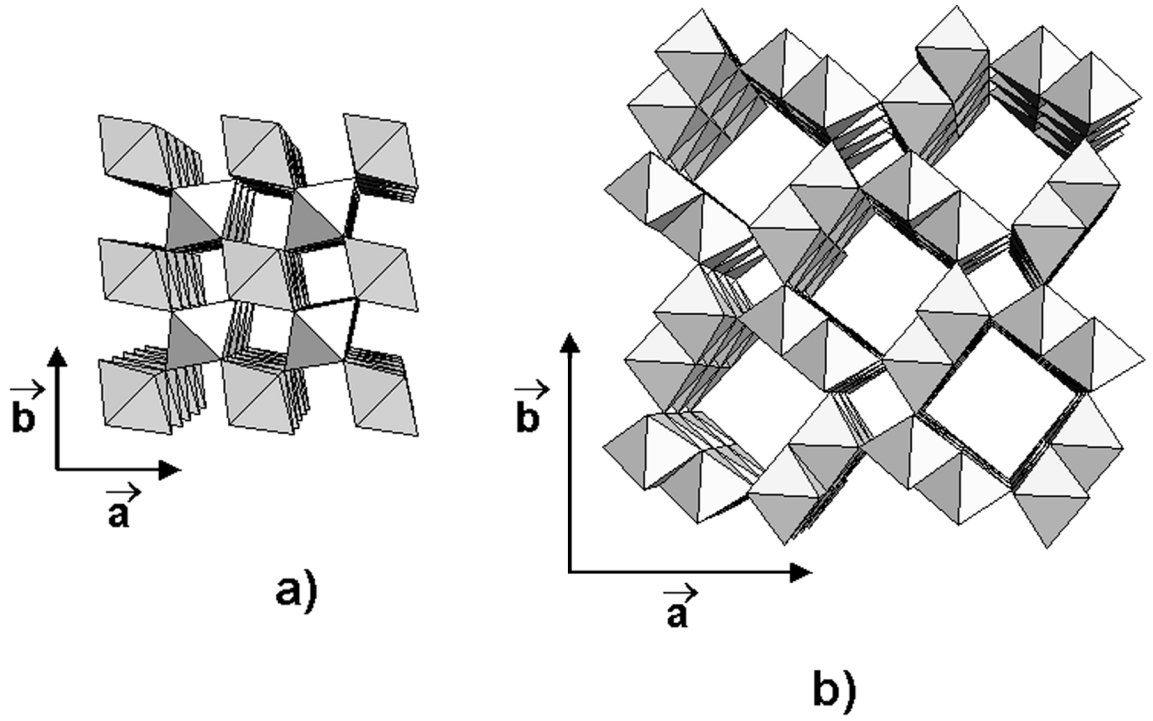


**Fig. 9** a) Rutile-type FeOF and b) open-structure hollandite-type 'FeOF·$nH_2O$' prepared in supercritical medium (sample A).

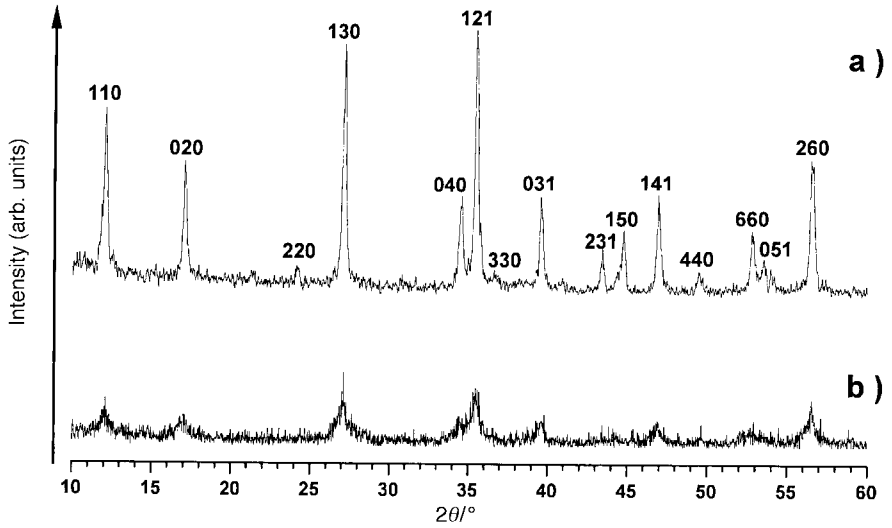


**Fig. 10** Powder XRD patterns of a) hollandite-type $FeOF_{1-x}(OH)_x \cdot nH_2O$ prepared in supercritical medium (sample A) and b) slightly fluorinated $\beta$-FeOOH prepared by the classical hydrolysis route (sample C).

(sample B), by hydrolysis of $FeCl_3$ as reported earlier;[62–64] and a slightly fluorinated hydrated iron oxyhydroxide (sample C), by hydrolysis of $FeF_3$.[60] This latter type of compound reveals a much lower crystallinity than those prepared in supercritical conditions, as shown in Fig. 10b.

In order to check the effectiveness of the oxidizing reaction and the final oxidation state of iron, samples obtained by supercritical treatment were treated afterwards under flowing HF at moderate temperatures ($40 < T < 150\,^{\circ}C$) for 2 hours. This type of fluorination reaction is known to be non-oxidative, and leads to an exchange of $O^{2-}$ and $OH^-$ anions by $F^-$. The phase obtained after reaction with HF corresponds to rhombohedral $FeF_3$ ($ReO_3$-derived phase), as characterized by XRD and EPMA. This result confirms that all $Fe^{2+}$ from $NH_4FeF_3$ had been fully oxidized to $Fe^{3+}$ during the reaction with $H_2O_2$ in supercritical $CO_2$–$H_2O$–ethanol.

The atomic ratios O/Fe and F/Fe have been estimated by EPMA and the fluorine and water contents have been obtained by DTA–TGA (under flowing nitrogen) coupled with mass spectrometry. The amount of water molecules depends on the conditions of the final $CO_2$ flow and varies from 0 to 0.4. In the case of sample A obtained as described above, the composition is $FeOF_{0.9}(OH)_{0.1}$.

The $FeOF_{1-x}(OH)_x \cdot nH_2O$ compounds were checked by infrared spectroscopy (diffuse reflectance), as well as hydrated β-FeO(OH,Cl) (sample B), as shown in Table 6.

The spectrum of sample B shows the characteristic bands of slightly chlorinated β-FeOOH, as reported earlier,[57,61,67] in particular those of the deformation mode of the Fe–O–Fe bonds ($\nu = 1070$–$1030\ cm^{-1}$), and the asymmetric and symmetric vibrations of Fe–O–Fe bonds at $\nu = 700$ and $420\ cm^{-1}$, respectively. Large quantities of water are also detected ($\nu =$ $3400$–$3300\ cm^{-1}$, $1620\ cm^{-1}$).

The spectra of the oxy(hydroxy)fluorides prepared in this work differ from those of chlorinated β-FeOOH: in addition to the Fe–O–Fe vibrations mentioned above and located at

**Table 6** Infared band assignments for $FeOF_{1-x}(OH)_x \cdot nH_2O$ and for slightly chlorinated iron oxyhydroxide (sample B) obtained by conventional hydrolysis of $FeCl_3$

| $FeOF_{1-x}(OH)_x \cdot nH_2O$ | | Type of vibration | Hydrated β-FeO(OH,Cl) (sample B) | |
|---|---|---|---|---|
| $\nu$/cm$^{-1}$ | Intensity (a.u.) | | $\nu$/cm$^{-1}$ | Intensity (a.u.) |
| 3500–3400 | s | $\nu$(OH) | 3480–3360 | vs |
| 3180 | s | Characteristic of fluorinated compound[a] | — | — |
| 1619 | mw | $\delta$(H–O–H) | 1615 | s |
| 1080 | w | Deformation modes of Fe–O(H)–Fe[61] | 1070 | vw |
| 1020 | m | | 1030 | w |
| 956 | m | Characteristic of fluorinated compound[a] | — | — |
| 845 | w | Interaction of $H_2O$ with hollandite tunnels[61] | 845 | m |
| 705 | ms | Asymmetric vibration of Fe–O–Fe in hollandite | 650–700 | ms |
| 424 | w | Symmetric vibration of Fe–O–Fe in hollandite | 420 | vw |

Intensities: vs = very strong; s = strong; m = medium; w = weak; vw = very weak. [a]These bands were assigned in previous works[57,61] to the signature of the presence of fluorine species in the structure.

$\nu$ = 1080–1020, 705, 425 cm$^{-1}$, two strong bands appear at $\nu$ = 3180 and 956 cm$^{-1}$. They were also found with much lower intensity in slightly fluorinated β-FeOOH,[57] and seem characteristic of fluorinated oxy-compounds. The amount of water present in the tunnels of sample A, which is in any case smaller than for sample B obtained *via* conventional hydrolysis, depends on the final $CO_2$ treatment. This may be related to the fact that flushing the reactor with the supercritical $CO_2$–ethanol mixture helps to eliminate residual water.[61] This is evident by the lowering of the intensity of the band at 845 cm$^{-1}$.

Electron diffraction and Rietveld refinement of powder X-ray diffraction data are in progress in order to elucidate the structural parameters of these new oxy(hydroxy)fluorides. A Mössbauer spectroscopy study will specify the oxidation state and the environment of iron. These results will be presented in a forthcoming paper.

## Conclusions

It has been pointed out that chemical synthesis in supercritical media is a new route for preparing either nanometric powders with narrow size distribution or oxy(hydroxy)fluorides exhibiting open frameworks.

As far as the formation of nanoparticles is concerned the following conclusions may be drawn. (i) The use of supercritical fluids as reactive medium allows control of the particle size distribution owing to the tunable density and solubility of the solute. Then the solute supersaturation can be continuously adjusted in order to control the size of the nanoparticles. The systematic variation of working conditions ($T$, $P$, solute supersaturation, hydrodynamics, *etc.*) and their effects on the particle size are under study. Thus, metallic nanoparticles prepared by this route should be very attractive for their size-dependent electrical, chemical, and magnetic properties. (ii) The nature of the final product depends on the nature of the solvent. The metallic atoms can easily react with ammonia, giving nitrides, $Cu_3N$ and $Fe_4N$, at temperatures clearly lower than those used in conventional solid state chemistry routes. (iii) The nature of the final product depends also on the nature of the metallic precursors (*e.g.* the formation of $Fe_2O_3$ results from the high reactivity of iron with oxygen present in acetylacetonate groups). In this case the preparation of pure metallic nanoparticles should require the use of metallic precursors free from oxygen. (iv) The supercritical chemistry route is interesting not only for obtaining either intimate homogeneous mixtures of nanoparticles, (*e.g.* $Fe_2O_3 + Fe_4N$) or metallic alloys (*e.g.* Cu–Pd), but also for the metallic coating of particles used as substrates and therefore insoluble in the supercritical fluid medium.

As far as the preparation of metastable phases is concerned: (i) the high diffusivity of $O^{2-}/OH^-$ species (in supercritical $CO_2$ medium) through the $NH_4FeF_3$ network coupled to the efficient elimination of water allows the synthesis of new types of compounds which adopt the hollandite-type structure with a framework exhibiting large tunnels; (ii) the phase corresponding to the $FeOF_{0.9}(OH)_{0.1}$ chemical composition shows a high fluorine content compared to fluorinated iron oxyhydroxides prepared by conventional routes.

The use of this method is now in progress for preparing other metastable phases with various transition metals, such as lamellar structures containing large interlayer spaces.

We are grateful to C. Chabot, L. Rabardel, E. Sellier and J. J. Videau for helpful discussions and technical support.

## References

1 N. B. Vargaftik, *Table on the thermophysical properties of liquids and gases*, Hemisphere Publishing Corporation, London, 1975.
2 *Innovations in Supercritical Fluids*, ed. K. W. Hutchenson and N. R. Foster, ACS Symp. Ser. 608, Washington DC, 1995.
3 *Supercritical Fluids—Fundamentals for Applications*, ed. E. Kiran and J. M. H. Levelt Sengers, NATO ASI Series E273, Kluwer, Dordrecht, 1994.
4 *Fluides Supercritiques et Matériaux*, ed. F. Cansell and J. P. Petitet, AIPFS Publishing, Nancy, France, 1995.
5 X. Y. Zeng, Y. Arai and T. Furuya, *Trends Chem. Eng*., 1996, **3**, 205.
6 P. G. Debenedetti, *Supercritical Fluids—Fundamentals for Application*, ed. E. Kiran and J. M. H. Levelt Sengers, NATO ASI Series E273, Kluwer, Dordrecht, 1994, pp. 719–729.
7 H. Ksibi and P. Subra, *Adv. Powder Technol*., 1996, **7**, 21.
8 K. Chhor, J. F. Bocquet and C. Pommier, *Mater. Chem. Phys*., 1995, **40**, 63.
9 P. Beslin, P. Jestin, Ph. Desmarest, R. Tufeu and F. Cansell, *Supercritical Fluids—Reactions, Material science and Chromatographiy*, ed. M. Perrut and G. Brunner, AIPFS Publishing Nancy, France, 1994, vol. 3, pp. 321–326.
10 R. A. Laudise and D. W. Johnson, *J. Non-Cryst. Solids*, 1986, **79**, 155.
11 B. Rangarajan and C. T. Lira, *J. Supercritical Fluids*, 1991, **4**, 1.
12 A. Akgerman and G. Madras, *Supercritical Fluids—Fundamentals for Application*, ed. E. Kiran and J. M. H. Levelt Sengers, NATO ASI Series E 273, Kluwer, Dordrecht, 1994, pp. 669–695.
13 *Supercritical Fluid Extraction: Principles and Practice*, ed. M. A. McHugh and V. J. Krukonis, Butterworths, Stoneham, MA, 1988.
14 F. Cansell, Ph. Botella, Y. Garrabos, J. L. Six, Y. Gnanou and R. Tufeu, *Polym. J*., 1997, **29**, 910.
15 E. J. Beckman, *Nature*, 1996, **271**, 613.
16 S. H. Page, J. F. Morrison and M. L. Lee, *Supercritical Fluids—Fundamentals for Application*, ed. E. Kiran and J. M. H. Levelt Sengers, NATO ASI Series E273, Kluwer, Dordrecht, 1994, pp. 641–652.
17 G. M. Schneider, *Fluid Phase Equilibr*., 1983, **10**, 141.
18 M. Poliakoff, M. W. Georges and S. M. Howdle, *Chemistry under extreme or non-classical conditions*, ed. R. V. Eldik and C. D. Hubbard, Wiley, New York, 1996, pp. 189–219.
19 P. Beslin, F. Cansell, Y. Garrabos, G. Demazeau, B. Berdeu and D. Sentagnes, *Déchets*, 1997, **5**, 17.

20 D. T. Chen, A. P. Craig, E. Reichert and J. Hoven, *J. Hazard. Mater*., 1995, **44**, 53.
21 H. Lentz and W. Mormann, *Makromol. Chem., Macromol. Symp*., 1992, **57**, 305.
22 K. P. Johnston, K. L. Harrison, M. J. Clarke, S. M. Howdle, M. P. Heitz, F. V. Bright, C. Carlier and T. W. Randolph, *Nature,* 1996, **271**, 624.
23 J. P. Petitet, *Fluides Supercritiques et Matériaux*, ed. F. Cansell and J. P. Petitet, AIPFS Publishing, Nancy, France, 1995, pp. 251–300.
24 C. A. Eckert, B. L. Knuston and P. G. Debenedetti, *Nature*, 1996, **383**, 313.
25 J. Chrastil, *J. Phys. Chem*., 1982, **86**, 3016.
26 P. E. Savage, S. Gopalan, T. I. Mizian, C. J. Martino and E. E. Brock, *AIChE J*., 1995, **41**, 1723.
27 F. Cansell, S. Rey and P. Beslin, *Rev. Inst. Fr. Pétrole*, 1998, **53**, 71.
28 J. W. Tom and P. G. Debenedetti, *J. Aerosol Sci*., 1991, **22**, 555.
29 D. W. Matson and R. D. Smith, *J. Am. Ceram. Soc*., 1989, **72**, 871.
30 H. Ksibi, P. Subra and Y. Garrabos, *Adv. Powder Technol*., 1995, **6**, 25.
31 B. Subramaniam, R. A. Rajewski and K. Snavely, *J. Pharm. Sci*., 1997, **86**, 885.
32 D. W. Matson, J. L. Fulton, R. C. Petersen and R. D. Smith, *Ind. Eng. Chem. Res.*, 1987, **26**, 2298.
33 E. Reverchon, *Supercritical fluids—Materials and natural products processing*, ed. M. Perrut and P. Subra, AIPFS Publishing, Nancy, France, 1998, pp. 221–236.
34 M. Poliakoff and M. W. George, *Supercritical Fluids: Materials and Natural Products Processing*, ed. M. Perrut and P. Subra, AIPFS Publishing, Nancy, France, 1998, pp. 833–842.
35 E. Dinjus, R. Fornika and M. Scholtz, *Chemistry under extreme or non-classical conditions*, ed. R. V. Eldik and C. D. Hubbard, Wiley, New York, 1996, pp. 219–272.
36 V. Gourinchas-Courtecuisse, K. Chhor, J. F. Bocquet and C. Pommier, *Ind. Eng. Chem. Res.*, 1996, **35**, 2539.
37 V. Gourinchas-Courtecuisse, J. F. Bocquet, K. Chhor and C. Pommier, *J. Supercritical Fluids*, 1996, **9**, 222.
38 Y. Hakuta, H. Terayama, S. Onai, T. Adschiri and K. Arai, *Supercritical Fluids—Chromatography and Novel Applications*, ed. S. Saito and K. Arai, AIPFS Publishing, Nancy, France, 1997, pp. 255–258.
39 T. Adschiri, S. Yamane, S. Onai and K. Arai, *Supercritical Fluids—Reactions, Material science and Chromatography*, ed. M. Perrut and G. Brunner, AIPFS Publishing, Nancy, France, 1994, vol. 3, pp. 241–246.
40 D. F. McLaughlin and M. C. Skriba, *US Pat*. 4,916,108, 1990.
41 F. Lu, S. Chen and S. Peng, *Catal. Today*, 1996, **30**, 183.
42 J. N. Armor and E. J. Carlson, *US Pat*. 4,615,736, 1986.
43 G. L. Schimek, W. T. Pennington, P. T. Wood and J. W. Kolis, *J. Solid State Chem.*, 1996, **123**, 277.
44 J. J. Watkins and T. J. McCarthy, *Chem. Mater*., 1995, **7**, 1991.
45 D. A. Loy, E. M. Russick, S. A. Yamanaka and B. M. Baugher, *Chem. Mater*., 1997, **9**, 2264.
46 B. N. Hansen, B. M. Hyberston, R. M. Barkley and R. E. Sievers, *Chem. Mater*., 1992, **4**, 749.
47 O. A. Louchev, V. K. Popov and E. N. Antonov, *J. Cryst. Growth*, 1995, **155**, 276.
48 V. K. Popov, V. N. Bagratashvili, E. N. Antonov and D. A. Lemenovski, *Thin Solid Films*, 1996, **279**, 66.
49 P. G. Debenedetti, *AIChE J.*, 1990, **36**, 1289.
50 S. K. Kumar, *J. Supercritical Fluids*, 1988, **1**, 15.
51 D. V. Baxter, M. H. Chisholm, G. J. Gama and V. F. DiStasi, *Chem. Mater.*, 1996, **8**, 1222.
52 H. Jacobs and J. Bock, *J. Less-Common Met*., 1987, **134**, 215.
53 R. Juza and H. Hahn, *Z. Anorg. Allg. Chem.*, 1939, **241**, 172.
54 S. Peter, F. Altofer, W. Bührer and H. D. Lutz, *VIth European Conference on Solid State Chemistry*, Zürich, Sept. 1997.
55 F. Kamoun, M. Lorenz, G. Kempe and F. Peger, *J. Less-Common Metals*, 1991, **170**, 1.
56 K. J. Gallagher and M. R. Ottaway, *J. Chem. Soc., Dalton Trans.*, 1974, 2347.
57 P. Keller, *N. Jb. Miner. Abh.*, 1970, **113**, 29.
58 P. Hagenmuller, J. Portier, J. Cadiou and R. de Pape, *C. R. Acad. Sci. Paris*, 1965, **260**, 4768.
59 M. Vlasse, J. C. Massies and G. Demazeau, *J. Solid State Chem.,* 1973, **8**, 109.
60 A. L. Mackay, *Mineral. Mag*., 1960, **32**, 545.
61 J. M. Gonzalez-Calbet, M. A. Alario-Franco and M. Gayoso-Andrade, *J. Inorg. Nucl. Chem.*, 1981, **43**, 257.
62 J. M. Combes, A. Manceau, G. Calas and J. Y. Bottero, *Geochim. Cosmochim. Acta,* 1989, **53**, 583.
63 R. Söderquist and S. Jansson, *Acta. Chem. Scand.*, 1966, **20**, 1417.
64 G. Biedermann and J. T. Chow, *Acta Chem. Scand.*, 1966, **20**, 1376.
65 J. E. Post and V. F. Buchwald, *Am. Mineral.*, 1991, **76**, 272.
66 M. Ohyabu and Y. Ujihira, *J. Inorg. Nucl. Chem.*, 1981, **43**, 3125.
67 E. Murad, *Clay Miner.*, 1979, **14**, 273.


*Paper 8/04964E*